OPEN ACCESS

University of BRISTOL

Temple, S., Roberts, N. W., & Misson, G. P. (2019). Haidinger's brushes elicited at varying degrees of polarization rapidly and easily assesses total macular pigmentation. *Journal of the Optical Society of America A*, *36*(4), B123-B131. https://doi.org/10.1364/JOSAA.36.00B123

Publisher's PDF, also known as Version of record

License (if available):
CC BY

Link to published version (if available):
10.1364/JOSAA.36.00B123

Link to publication record in Explore Bristol Research
PDF-document

This is the final published version of the article (version of record). It first appeared online via The Optical Society at https://doi.org/10.1364/JOSAA.36.00B123 . Please refer to any applicable terms of use of the publisher.

University of Bristol - Explore Bristol Research

General rights

This document is made available in accordance with publisher policies. Please cite only the published version using the reference above. Full terms of use are available:
http://www.bristol.ac.uk/pure/about/ebr-terms

Research Article Vol. 36, No. 4 / April 2019 / Journal of the Optical Society of America A B123

Journal of the Optical Society of America A

OPTICS, IMAGE SCIENCE, AND VISION

Haidinger's brushes elicited at varying degrees of polarization rapidly and easily assesses total macular pigmentation

Shelby E. Temple,[1,2,*] Nicholas W. Roberts,[2] and Gary P. Misson[3,4]

[1]School of Biological Sciences, University of Bristol, Bristol BS8 1TQ, UK
[2]Azul Optics Ltd, Bristol BS10 5BD, UK
[3]School of Life and Health Sciences, Aston University, Birmingham B4 7ET, UK
[4]South Warwickshire NHS Foundation Trust, Warwick Hospital, Lakin Road, Warwick CV34 5BW, UK
*Corresponding author: shelbytb@hotmail.com

Received 20 November 2018; revised 6 March 2019; accepted 7 March 2019; posted 8 March 2019 (Doc. ID 352122); published 27 March 2019

Macular pigments (MPs), by absorbing potentially toxic short-wavelength (400–500 nm) visible light, provide protection against photo-chemical damage thought to be relevant in the pathogenesis of age-related macular degeneration (AMD). A method of screening for low levels of MPs could be part of a prevention strategy for helping people to delay the onset of AMD. We introduce a new method for assessing MP density that takes advantage of the polarization-dependent absorption of blue light by MPs, which results in the entoptic phenomenon called Haidinger's brushes (HB). Subjects were asked to identify the direction of rotation of HB when presented with a circular stimulus illuminated with an even intensity of polarized white light in which the electric field vector was rotating either clockwise or anti-clockwise. By reducing the degree of polarization of the stimulus light, a threshold for perceiving HB (degree of polarization threshold) was determined and correlated ($r^2 = 0.66$) to macular pigment optical density assessed using dual-wavelength fundus autofluoresence. The speed and ease of measurement of degree of polarization threshold makes it well suited for large-scale screening of macular pigmentation.

Published by The Optical Society under the terms of the Creative Commons Attribution 4.0 License. Further distribution of this work must maintain attribution to the author(s) and the published article's title, journal citation, and DOI.
https://doi.org/10.1364/JOSAA.36.00B123

1. INTRODUCTION

Macular pigments are xanthophyll carotenoids of dietary origin. Of the 600 or more carotenoids found in nature, and 40–50 found in the human diet [1], only lutein, zeaxanthin, and meso-zeaxanthin are concentrated in a dense layer in the inner retina directly over the macula, where they intercept the path of light before it reaches the photoreceptors. The macular pigments (MPs) absorb up to 70% of the short-wavelength (400–500 nm, violet/blue) light that enters the eye [2]. As these short wavelengths are more highly scattered than longer wavelengths, MPs reduce the impact of chromatic aberration from the ocular media as well as the deleterious effects of glare, resulting in improved contrast sensitivity [3–7]. Based on both their well-established antioxidant behavior [8] and their ability to decrease violet/blue light reaching the retina [9], MPs are thought to protect the retina from accumulation of photochemical damage [10]. The protective nature of MPs is supported by their localization in the area of the retina with the least vascularization yet the highest metabolic rate of any part of the central nervous system [11]. The macula benefits from the ability of MPs to quench reactive oxygen species generated photochemically, metabolically, and arriving as toxins from poor diet or other insults such as smoking [2,10]. Low levels of MPs have therefore been implicated in long-term accumulation of photochemical damage [12] and with increased likelihood of developing age-related macular degeneration (AMD) [13–19]. A method of assessing macular pigment density (MPD) that is suitable for mass screening could provide a valuable tool for informing people of their natural levels of protection so that they can be empowered to take preventative actions to further protect their eyes from violet/blue light and reduce other risk factors including smoking [20,21] and obesity [22,23].

Various techniques have been developed to indirectly assess MPD *in vivo* by measuring a variable that has been correlated with MPD such as the strong absorption of short-wavelength light by MPs. Measurements are made by comparing differential absorbance/reflectance at wavelengths above and below 520 nm

made for an area where MPD is high compared to an area where MPD is low (the latter providing a baseline that accounts for losses due to the optics of the eye). Techniques are either physical (objective, using an optical sensor outside the eye) or psychophysical (using the retina as the sensor and the individual's subjective response), and all rely on various assumptions about the underlying optics of the eye or behavior of the subject (reviewed in [24]). Physical techniques typically require pupil dilation to improve image acquisition but often provide the advantage of giving a two- or even three-dimensional image of the MPD across the macula. Psychophysical techniques typically only measure at one point/eccentricity in the macula at a time and therefore require numerous measurements to assess the total MPD, but they often have the advantage of being easier and quicker to perform and better suited to mass screening in clinical settings.

Recently, an entirely new method of assessing MPD was proposed [25] that is based on the differential absorbance of polarized light by the MPs [26], which is central to the underlying mechanism responsible for the perception of the entoptic phenomenon known as Haidinger's brushes [27,28]. This psychophysical approach uses the subjects' threshold for detecting Haidinger's brushes (HB) as the degree of polarization (DoP) is decreased to assess the total amount of MP in the macula (see the Theory section below). The technique does not require pupil dilation and can be performed on anyone with normal vision irrespective of refractive error or astigmatism. HB is accommodation independent because it is the shadow on the retina of the MPs themselves, which are immediately anterior to the retina in the path of light after it has passed through the optic media. The technology required to deliver the test is inexpensive and can be packaged into a compact housing, which combined with ease of use and the short time needed for the test would make it suitable for optometric or clinical use.

As a part of the process of validating this new technique, we compared the repeatability and time requirements for different testing protocols for measuring the degree of polarization threshold in both a research and a clinical setting. We also compared degree of polarization threshold to macular pigment optical density (MPOD) measured using dual-wavelength fundus autofluorescence.

2. THEORY AND METHODS

A. Theory

Theoretical studies [28–31] have shown that HB can be modeled by assuming that the macula acts as a radially symmetric diattenuator. This is based on the molecular arrangement of the macular pigments that are oriented, on average, normal to the plane of the cell membranes [32] of the photoreceptor axons that form the Henle fiber layer [27]. These axons radiate outwards from the center of the fovea like the spokes of a wheel. Thus, for any angle of polarization (AoP) of incoming linearly polarized light, the light transmitted though the radial diattenuator (the macula) varies throughout a circle in accordance with Malus's law. This pattern has the form of HB with maximum transmittance (k_1) along a radius from the center of the radial diattenuator parallel to the plane of the AoP and a minimum transmittance (k_2) along a radius from the center of the radial diattenuator perpendicular to the plane of the AoP (Fig. 1).

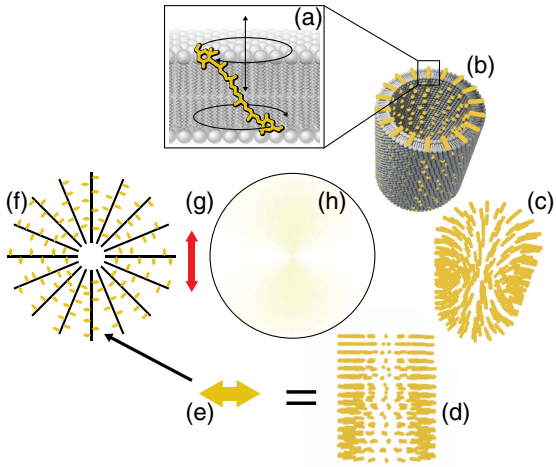

Fig. 1. Schematic description of how the orientation of macular pigments leads to the perception of the Haidinger's brushes phenomenon. Average orientation of (a) macular pigment molecules in the cell membrane is normal to the surface of the lipid bilayer [32]. This orientation leads to macular pigments being oriented radially relative to (b) the cylindrical shape of the axons of the photoreceptors in the Henle fiber layer, made more apparent by (c) and (d) the removal of the lipid bilayer. The average alignment of the macular pigments is therefore at right angles to the axon when observed side-on (d), resulting in a net orientation (e) perpendicular to the long axis of the axons (f) that radiate out from the center of the fovea. The absorption of polarized light with (g) its electric field vector oriented vertically by the short-wavelength absorbing and diattenuating macula will be maximum in areas of the macula where the MPs are aligned with the orientation of the electric field vector (minimum transmittance = k2). And absorption will be minimum in areas of the macula where the MPs are aligned perpendicularly with the orientation of the electric field vector (maximum transmittance = k1). This pattern of absorption results in (h) a yellow shadow on the retina in the shape of a bowtie or hour-glass known as Haidinger's brushes that rotates when the electric field vector rotates (see Visualization 1).

The corneal stromal layers cause the cornea to act like a birefringent anisotropic crystal, effectively converting linearly polarized light into elliptically polarized light. The magnitude of this corneal retardation also affects HB contrast; however, there are four orientations of incoming linear polarization (fast/slow retardation axes when the intrinsic ocular retardation has zero effect. The confounding effect of intrinsic ocular birefringence is therefore eliminated by continuously rotating the incident linear polarized light such that HB will have maximum contrast four times per cycle. Rotation also favors the perception of HB by overcoming any tendency of the retina to adapt to an otherwise fixed image (Troxler effect), which explains why the HB phenomenon vanishes rapidly when observed against a static polarized light field. These points are important when determining a threshold of perception of HB as in this study.

The salience of a rotating HB is dependent on the degree of polarization of incident light, the difference between the maximum and minimum transmittances ($k_1 - k_2$) of the macular radial diattenuator, and the absolute extent to which the macula absorbs polarized light here related to the density of macular

pigment at any given point on the macular radial diattenuator. This is expressed as a difference of resultant transmittances $\Delta I = D_m \times \mathrm{DoP} \times (k_1 - k_2)$, where D_m is the normalized MPD. If it is assumed that there is complete maximum transmission ($k_1 = 1$) [28] and that k_2 and D_m are constant, there will be a threshold degree of polarization (T_{DoP}) at which ΔI is sufficiently large for HB to be perceived such that

$$T_{\mathrm{DoP}} = \frac{\Delta I}{D_m(1 - k_2)}. \quad (1)$$

There are no published absolute transmittance values; however, for the present study we use $k_2 = 0.91$ obtained from the average ratio $k_1/k_2 = 1.1$ for humans *in vivo* [33] and the simplifying assumption that $k_1 = 1$.

The underlying assumptions for assessing MPD with the degree of polarization threshold are: (1) that the orientation of the MPs is on average normal to the lipid bilayer of the cell membranes of the photoreceptor axons, which is supported by empirical studies [11,32,34]; (2) that the normal Henle fibers have a radiating structure; (3) that the distribution of MPs is radially symmetrical; and (4) that the macular retina has normal function (see the following list). Disease states known to interfere with the observation of HB [35,36] will obviate the ability to assess MPD with the degree of polarization threshold, e.g., macular damage due to diabetes or AMD, macular oedema, amblyopia, photoreceptor dysfunction such as color blindness, and opacities of the ocular media. As such, the inability to perceive HB during a test for the degree of polarization threshold could be used as a method of screening for any of the above visual dysfunctions.

B. Instrument Design

The core technology underlying degree of polarization threshold testing was developed for the purposes of investigating the lower limit of DoP at which cuttlefish and octopus could detect AoP contrast. Cephalopods are colorblind and use polarization, much as we use color, to parse images of their surroundings. To extend findings of their remarkably acute polarization vision [37,38], new technology was developed to adjust the DoP with custom-made depolarizing filters. The depolarizing filters were made by mixing hollow glass spheres into polyester resin at different densities, whereby increasing the density of glass spheres decreased the DoP of the light transmitted. These filters combined with a rotating polarizer, a technique that has been used to generate sustained perception of Haidinger's brushes for at least 150 years [39], form the core elements of the degree of polarization threshold approach.

White light for the stimulus (see Appendix A for spectral output) is generated by a flat-panel LED placed behind a polarizer rotating either clockwise of counter-clockwise at 60 rpm, driven by a stepper motor. A filter wheel containing 10 custom-made depolarizing filters is controlled by a second stepper motor to position any one of 10 filters between the rotating polarizer and the subject's line of sight. The subject views the stimulus through a series of apertures, which are illuminated by a second LED with identical spectral output to that used for the stimulus. The light conditions thus created optimize perception of HB and remove potential intensity artifacts that could be used to determine the direction of rotation (Fig. 2).

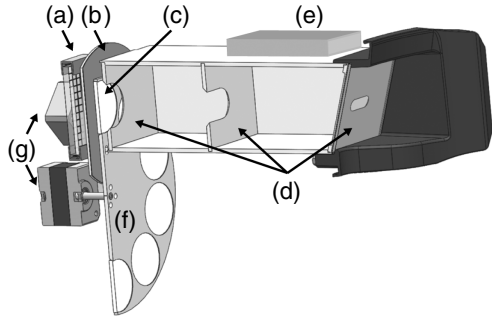

Fig. 2. Schematic diagram of the optical components for the degree of polarization threshold testing device. (a) A custom-built LED panel produces white light that is polarized by a (b) rotatable linear polarizing filter before being transmitted through (c) a custom-made degree of polarization (DoP) filter. (d) A series of apertures reduce the path of light to a narrow angle to stop light reflected from flat surfaces reaching the subject's eye. (e) A second LED panel identical to (a) is used to diffusely illuminate the viewing tube. Different DoP values can be presented by rotating through (f) a series of filters mounted in a carousel. (g) Stepper motors drive the rotation of both the polarizer and the carousel.

C. Degree of Polarization Threshold Testing

To determine the degree of polarization threshold, the subject was given a brief description of how best to observe HB and shown a simulation of how HB would appear [giving an accurate representation of rate of rotation (60 rpm), approximate size, and shape of the effect; see Visualization 1], followed by practice observations. The subject was instructed to use both eyes to look into the center of the stimulus and to try not to focus on the plane of the stimulus but rather to accommodate at infinity as if looking at a cloud far away. They were informed that their personal perception of HB may be less salient (less strongly colored) than the simulation, because the effect was due to the shadow created by their own macular pigments on their retina and that a lower MPD would result in a weaker effect. It was, therefore, not possible to simulate precisely how each individual would perceive the effect. The subject was informed that they would be asked to correctly identify the direction of rotation for numerous presentations of HB and that the effect would, in some instances, be impossible to perceive. They were instructed not to guess (except in the forced choice protocol described below), but rather to do their best to get a sense of rotation direction from the effect even when it was extremely faint. The subject was then asked to position themselves such that they could see the stimulus with both eyes through the series of apertures (Fig. 2). The subject was then shown the stimulus with the highest DoP (easiest setting) and asked to identify the rotation direction verbally or by moving their finger in the air or on the table in the direction of rotation. The test was then commenced. Three different psychophysical methods (protocols) were used for determining a subject's degree of polarization threshold as described below. Informed consent was obtained from all subjects, and the testing was in accord with the tenets of the Declaration of Helsinki. All participants had normal vision with no known eye disease.

It should be noted that for nearly all MPD metrics, test results are based on a comparison between two measurements:

one made within the macula where MP density is high and one made at a perifoveal location where MPD is very low (peripheral baseline or background). HB-based approaches do not require a peripheral baseline because the HB effect rotates around the entire macula such that the same regions are used for both measurement and baseline but are separated temporally.

Protocol 1 involved a pseudorandomized order of DoP filter presentation using a binomial forced-choice paradigm. In this randomized approach, subjects were shown 120 presentations (12 for each of 10 different DoP filters) in pseudorandom order (could not be presented with the same DoP level more than twice in a row to reduce potential changes in subject motivation state if several easy or difficult stimuli were repeatedly presented) and asked to determine the direction of rotation or give a best guess for every presentation. A subject's degree of polarization threshold was determined as the minimum DoP at which the subject correctly identified the direction of rotation on at least nine of twelve presentations, which gives an estimated cumulative probability of 98%. This protocol was compared to an established physical method of assessing MPOD using dual-wavelength fundus autofluorescence (2WAF; described below). Subjects for the first protocol included 9 men and 11 women with a mean age of 44 (range 27–69).

Protocol 2 used a descending-only method of limits approach. An ascending-descending or staircase method was found to be unsuitable for testing of degree of polarization threshold because the appearance of a central yellow shadow that matches the description of Maxwell's spot [40] is formed when DoP is low and seems to make observing the rotation direction of HB on the ascending approach difficult and inconsistent. The disappearance of HB on the descending approach, however, is highly consistent as evidenced by repeatability results (see below). For the descending-only method of limits approach, degree of polarization threshold was determined as the minimum DoP achievable in three out of five descents. If, as was frequently the case, the same DoP was achieved in the first three descents, no further descents were required. This protocol was compared to MPOD measured using 2WAF. Subjects for the second protocol included 8 men and 6 women with a mean age of 44 (range 28–71).

Protocol 3 was a single-descent approach in which subjects were not forced to choose a rotation direction for every presentation. Subjects were asked not to guess but to try as hard as they could to determine the rotation direction based on any perception of movement in the HB phenomenon and to state when they were unable to detect the rotation. This protocol was developed through numerous iterative trials with subjects (not described here), which resulted in a simple testing regime that included the potential for second attempts for failed responses if preceding responses were received within 10 s (this only occurred on rare occasions). If more than two second attempts were required, the trial was stopped and recommenced and the subject asked not to guess. The test was controlled by custom-programmed Android-based software that tracked the time taken for each subject to respond after the presentation of each stimulus. Subject testing was performed by four optometrists in their clinics. Anonymized data was collected from 168 subjects.

D. Dual-Wavelength Fundus Autofluorescence

MPD was assessed for subjects in both the first and second degree of polarization threshold protocols using a 2WAF approach (Spectralis HRA + OCT MultiColor, Heidelberg Engineering GmbH, Heidelberg, DEU). This objective physical measurement approach employs confocal scanning laser ophthalmoscopy (cSLO) imaging with lasers at two excitation wavelengths: 486 nm, which is strongly absorbed by macular pigments, and 518 nm, which is weakly absorbed by macular pigments. Digital images were taken at both wavelengths and processed using the Heidelberg Eye Explorer software (HEYEX, version 1.7.1), from which a macular pigment density map was created. MPOD values were obtained at 0.23°, 0.50°, 0.98°, and 1.76° eccentricity as well as an estimate of volume calculated as the area under the curve out to an eccentricity of 7°. Peripheral baseline measurements were acquired at 7° eccentricity. A more comprehensive description of this technique can be found in [41].

E. Test-Retest

Repeatability of the degree of polarization threshold approach was tested for both the descending-only method of limits approach and the single-descent approach using a different sample population. For the descending-only method of limits approach, 17 subjects, 2 men and 15 women took part in the study. Age was not recorded. For the single-descent approach, 32 subjects, 24 men and 8 women with a mean age of 45 (range 8–74) took part in the study. None of the subjects reported any ocular disease or dysfunction. Each subject was given brief instructions and observed the simulation of the appearance of the effect as described previously. Retesting was conducted usually on the same day under identical conditions. All tests were carried out by one operator.

F. Statistical Analysis

All plots and statistics were done using SPSS v23 and Microsoft Excel 2010. Comparisons between degree of polarization threshold and MPOD as measured with 2WAF were made using the nonlinear regression to the model generated based on Eq. (1) in which MPOD values are multiplied by a machine-dependent scaling factor (μ) to convert them to normalized macular density values (D_m). k_2 was fixed at 0.91 (see Section 2.A), and ΔI and μ were optimized using least-squares fitting.

3. RESULTS

The amount of time required for each of the three protocols for testing degree of polarization threshold differed considerably. The binomial forced-choice approach took the longest to perform, with subjects requiring 17 min on average (range 8–42 min, $n = 20$) to complete the 120 observations. The descending-only method of limits approach took on average 6 min 30 s (range 2–14 min, $n = 14$). The single-descending-pass approach took an average of 53 s (range 16–218 s, $n = 168$). This time did not vary significantly (Kruskal-Wallis H test $\chi^2(3) = 6.67$, $p = 0.08$) between the populations sampled by each optometrist (61, 57, 44, and 62 s) allowing the data to be combined as a single data set (Fig. 3). The mean degree of polarization threshold value for the London-based sample

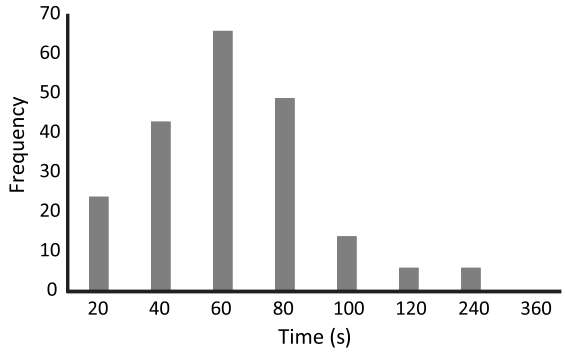

Fig. 3. Frequency histogram of time taken for degree of polarization threshold measurements in clinical settings using the single-descending-pass approach. Four optometrists used our device in their practices and measured the degree of polarization threshold on their patients ($n = 168$). Mean time to acquire a measure of degree of polarization threshold was 53 s (range 16–218 s).

population was 0.75 and did not vary significantly [$\chi^2(3) = 2.37$, $p = 0.50$] between the populations sampled by each optometrist. The combined data is presented as a single plot in Fig. 4.

The mean difference in the test-retest degree of polarization threshold values for the descending-only method of limits approach was 4.20×10^{-2}, and the limits of agreement (mean ± 1.96 SD) were $4.20 \times 10^{-2} \pm 7.34 \times 10^{-2}$, providing a coefficient of repeatability of 0.143 or 14.3% [Fig. 5(a)]. The mean difference in the test-retest degree of polarization threshold values for the single-descent approach was 5.00×10^{-3}, and the limits of agreement (mean ± 1.96 SD) were $5.00 \times 10^{-3} \pm 6.10 \times 10^{-2}$, providing a coefficient of repeatability of 0.119 or 11.9% [Fig. 5(b)].

Degree of polarization threshold was compared to MPOD volume and to MPOD at various eccentricities from the center of the fovea, measured using 2WAF. The theoretical model [Eq. (1)] that predicted an asymptotic nonlinear relationship provided a better fit to the comparison between degree of polarization threshold and MPOD than a linear relationship [MPOD volume versus the binomial forced-choice approach, nonlinear $r^2 = 0.43$ versus linear $r^2 = 0.39$ [Fig. 6(a)]; MPOD volume versus degree of polarization threshold descending-only method of limits approach nonlinear $r^2 = 0.62$ versus

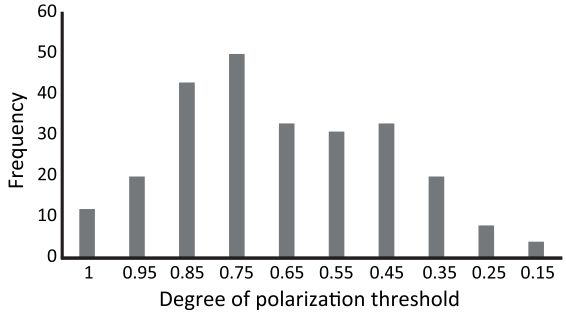

Fig. 4. Distribution of the degree of polarization threshold values for 168 patients measured in four optometry practices during regular eye exams.

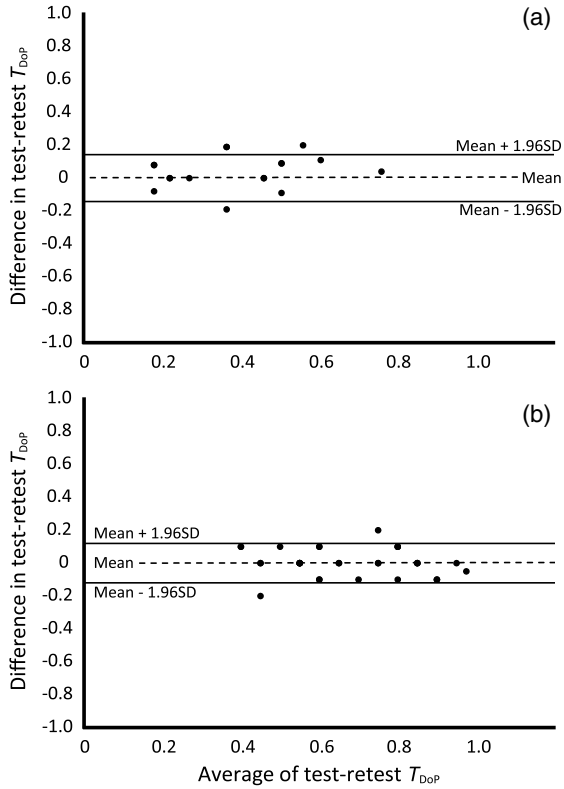

Fig. 5. Bland Altman plots for the (a) descending-only method of limits approach and (b) the single-descent approach, showing the difference in test-retest degree of polarization threshold values versus the average of the two degree of polarization threshold values. In both cases (a) and (b), the mean difference (dashed line) was zero, indicating no consistent change in score between the test and retest. The limits of agreement (solid horizontal lines) indicate the 95% confidence intervals.

linear $r^2 = 0.45$ [Fig. 6(b)]. Subsequent comparisons were made with the nonlinear model only. Good correlations were also observed between degree of polarization threshold values measured using the binomial forced-choice approach and MPOD at 1.75° and 1.0° eccentricities ($r^2 = 0.49$ and $r^2 = 0.54$, respectively; Table 1), as well as for degree of polarization threshold measured using the faster descending-only method of limits approach at 1.75°, 1.0°, and 0.5° eccentricities ($r^2 = 0.44$, $r^2 = 0.66$, and $r^2 = 0.42$ respectively; Table 1).

The correlation between MPOD volume and MPOD at specific eccentricities, both measured with 2WAF, increased with increasing eccentricity from $r^2 = 0.61$ at 0.25° eccentricity to $r^2 = 0.83$ at 1.75° eccentricity (Table 1).

4. DISCUSSION

The relationship between degree of polarization threshold and MPD was modeled [Eq. (1)] and found to be nonlinear, reaching an asymptote at a degree of polarization threshold value greater than zero as MPD increased (Fig. 7). This relationship reflects the underlying retinal origins of the HB entoptic phenomenon [27], which is dependent on the density of macular pigments. The model predicts that at low MPD

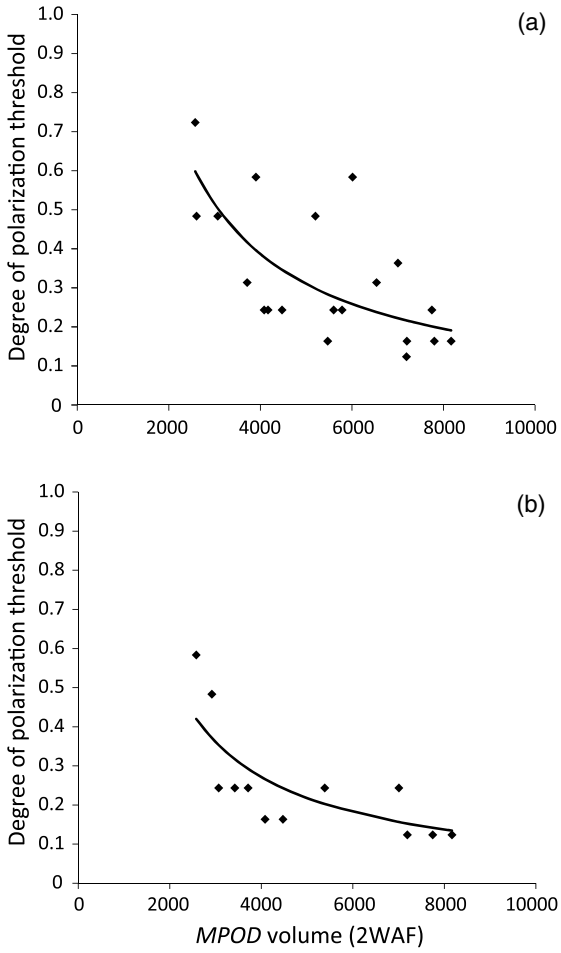

Fig. 6. Correlation between macular pigment optical density (MPOD) measured as volume by dual-wavelength fundus autofluorescence (2WAF) and degree of polarization threshold measured using (a) the binomial forced-choice approach ($r^2 = 0.43$) and (b) the descending-only method of limits approach ($r^2 = 0.62$). The model was fit with nonlinear least-squares regression.

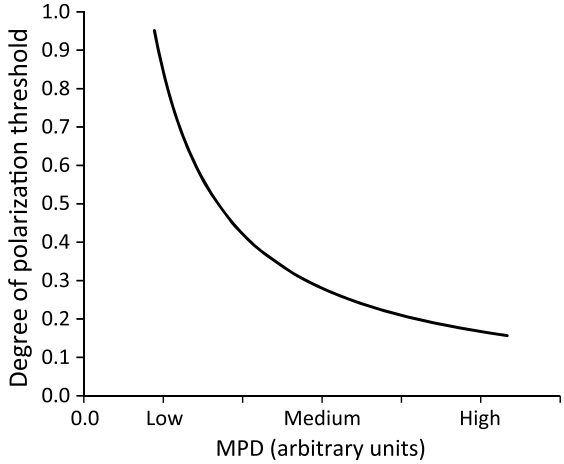

Fig. 7. Theoretical model to predict degree of polarization threshold (T_{DoP}) relative to the density of macular pigment MPD in the macula as per Eq. (1), where k_2 was set to 0.91, ΔI was 0.2, and the scaling constant μ was set to 0.0017. Note that MPD has been given arbitrary units as there are numerous measures of MPOD and the relationship is predicted to apply to any such comparison provided the measure of MPD reflects the total amount of pigment in the macula.

the degree of polarization threshold is limited by the contrast in the yellow shadow created by HB being below the threshold for detection. As MPD increases, the degree of polarization threshold decreases, reflecting the increased contrast created by greater absorption by the MPs that results in an increased salience of HB and therefore an increased ability to perceive HB at lower DoP. Towards the upper end of MPD, the degree of polarization threshold gradually approaches a theoretical minimum necessarily greater than $T_{DoP} = 0$, at which point there would be insufficient contrast with which to detect the direction of rotation of HB. The model was tested by comparing measurements of the degree of polarization threshold and MPOD within the same subjects. The nonlinear model gave a better fit to the comparisons between the degree of polarization threshold and MPOD than a straight line.

Table 1. Correlation of Degree of Polarization Threshold (T_{DoP}) with Macular Pigment Optical Density (MPOD) Measured by Dual-Wavelength Autofluorescence (2WAF)[a]

MPOD Dual-Wavelength Autofluorescence (2WAF)					
Eccentricity	**0.25°**	**0.50°**	**1.00°**	**1.75°**	**Volume**
T_{DoP} binomial forced choice	−0.08	0.05	0.54	0.49	0.43
T_{DoP} descending-only method	0.31	0.42	0.66	0.44	0.62
MPOD 2WAF volume	0.61	0.76	0.83	0.83	1.00

[a]Values are reported as r^2; see methods for calculations.

Correlation between the different protocols for measuring the degree of polarization threshold and MPD [Figs. 6(a) and 6(b), Table 1] support the previous hypothesis of a relationship between the degree of polarization threshold and MPD [25]. Muller *et al.* [42] also demonstrated a good correlation between their HB technique (HB visibility) and MPOD when measured as volume in the central 4° using 2WAF. The correlation between the degree of polarization threshold and different measures of MPOD was best (r^2 of 0.44–0.66) for measures of volume and at single eccentricities greater than 0.5°, when measured with 2WAF. The good correlation between the degree of polarization threshold and volume, or single eccentricities greater than 0.5°, may reflect the nature of the HB phenomenon as used here, which requires that the subject be able to detect the direction of rotation, a task that requires not only enough contrast in HB but also a shape of HB that is large enough to follow. These factors and our results suggest that the degree of polarization threshold approach is well suited to assessing the total amount of MP in the macula. Similarly, the correlation between MPOD volume and MPOD measured at single eccentricities also improved as eccentricity increased from 0.25° to 1.75° when measured by 2WAF (Table 1). We found that single measures at 0.25° and 0.5° eccentricity were less strongly correlated to total volume of MP than single measures at 1.0° and 1.75° (Table 1). This is logical given the increased volume of MP accumulating as the diameter of the

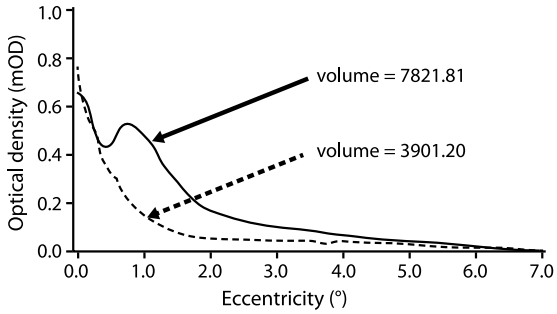

Fig. 8. Difference in total macular pigment (volume) for two individuals with similar macular pigment optical density values at eccentricities below 0.5°. Measurements made using dual-wavelength autofluorescence.

sampling area effectively increases and suggests that if a measure of MPOD at a single eccentricity was used to assess the total amount of MP in the macula, such a measurement should be made at an eccentricity greater than 1.0° but less than 3°. Furthermore, the shape of the MPD profile is not a simple exponential decrease as eccentricity increases away from the center of the macula, as was once suggested based on HFP measurements [43,44], but rather the pattern of MPD with eccentricity varies between individuals from peaked in the center to a central dip or ring-like profile [45–47]. This means that a single measure of MPOD at an eccentricity of 0.5° could be the same for two subjects despite their total volume of MP differing by nearly two-fold (e.g., Fig. 8). The implications of these different shapes on retinal health is an active area of investigation [48,49].

The lack of perfect agreement between any two methods of assessing MPD has been a consistent theme in the context of the introduction of new assessment techniques [41,43,50–52] and has not been aided by the lack of a "well-defined global metric" [52]. This reflects the fact that all available *in vivo* techniques do not directly measure MPD but rather make one of a variety of different measurements that have been proposed to be correlated with MPD, and each has its own underlying assumptions (reviewed in [24]). The correlation between degree of polarization threshold and MPD found here, which was as high as $r^2 = 0.66$, compares well with other studies that have compared highly varied techniques like resonance Raman spectroscopy and HFP ($r = 0.467$) [53] and single-wavelength reflectance and 2WAF ($r^2 = 0.047$) [54]. Comparisons between more similar techniques, like two different methods of HFP, provided a correlation of $r^2 = 0.46$ [50], and direct comparisons at the same eccentricities between 2WAF and HFP have provided correlations of 0.87, 0.85, 0.71, and 0.42 (using Lin's Concordance Correlation Coefficient, CCC) for 0.25°, 0.50°, 1.0°, and 1.75°, respectively [54].

In order to determine the sensitivity of the degree of polarization threshold technique for detecting changes in MPD over time, we measured the repeatability of two approaches for measuring degree of polarization threshold. The coefficient of repeatability of the descending-only method of limits was 0.143 or 14.3%, which equates to just greater than one DoP filter on the device, which has DoP filters spaced at 10% intervals. The faster single-descent method gave a coefficient of repeatability of 0.119 or 11.9%, which compares well with repeatability measured on other psychophysical devices (Macular Metrics, Macular Densitometer at 0.11–0.12 [50] and 0.19–0.21 [44] and Elektron Technologies, MPSII/Quantifeye at 0.18–0.21 [50] and 0.28–0.33 [55]). Given the primary objective of this rapid MPD assessment tool to categorize patients into high, medium, or low MPD levels in order to provide them with advice around how to protect their vision, the ability to repeatedly obtain a degree of polarization threshold score within one filter is appropriate. For tracking changes in MPD over time, one must consider that changes would need to be greater than 11.9% to be above the level of uncertainty.

The degree of polarization threshold approach is not a replacement for existing MPD assessment techniques, which typically provide more detailed information about MPOD in specific locations across the macula and which are already established as methods in long-term research studies. But the degree of polarization threshold approach may provide an effective screening tool to rapidly and easily assess MPD in clinical or even home settings. Degree of polarization threshold screening could enable eye care professionals to give patients advice about preventative actions that they could take to help compensate for reduced levels of protection offered when their MPD is low. The role of MPs in protecting the eye over a lifetime comes from their short-wavelength absorbing properties that reduce retinal levels of high-energy short-wavelength violet/blue light (<500 nm), which is well known to causes photochemical damage to the retina (reviewed in [10]) such as the long-term damaging effects of sunlight exposure [56–59]. Preventative actions for patients with low MPD could include avoiding direct or reflected exposure to sunlight, wearing a hat, sunglasses, having blue-blocking lens coatings on prescription glasses, maintaining or increasing MPD by eating a diversity of foods containing lutein and zeaxanthin or supplementing the diet with alternate sources of the macular carotenoids, quitting smoking, and losing weight [60–64]. In addition, degree of polarization threshold screening could be used to determine which patients should be further investigated with more in-depth analyses.

The ease and speed of degree of polarization threshold measurement, along with its repeatability, make this technique ideally suited for assessing total macular pigment levels in patients in primary eye care facilities. The simplicity of the testing procedure lends itself to operation by less qualified staff and can be set up to allow subjects to test themselves. The simplicity of the task for the subject suggests that the system would be well suited for screening children, which would enable eye care professionals to provide advice around protection from blue light early in life when the high violet/blue light transparency of the lens and cornea at these ages [65] put the retina at most risk. The establishment of degree of polarization threshold measurements as part of regular eye exams would help to inform patients of their increased risk to long-term damage from violet/blue light so that they could take preventative actions to delay the onset of accumulative photochemical damage of the type that is associated with AMD.

APPENDIX A

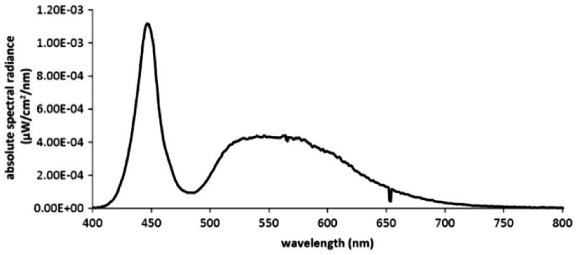

Fig. 9. Absolute spectral radiance of the stimulus and background LED. Measured with a USB 2000 spectroradiometer (Ocean Optics, California). Note that the stimulus LED was powered at half power, and this measurement was made at full power.

Figure 9 shows the spectral output of the LEDs' white light, as mentioned in Section 2.B (Instrument Design).

Funding. Innovate UK (900042); Engineering and Physical Sciences Research Council (EPSRC) (EP/M000885/1); Biotechnology and Biological Sciences Research Council (BBSRC) (Impact Acceleration Award).

Acknowledgment. The authors are grateful to John Nolan, Rachel Moran, and Rebecca Powers from the Macular Pigment Research Group of Waterford Institute of Technology for Spectralis data collection; Matthew Evans and Joseph Cefai of Azul Optics Ltd for technical support; and the optometrists and subjects that graciously agreed to participate in the study. S. E. T. acknowledges the support from Innovate UK and BBSRC.

REFERENCES

1. F. Khachik, G. R. Beecher, M. B. Goli, and W. R. Lusby, "Separation, identification, and quantification of carotenoids in fruits, vegetables and human plasma by high-performance liquid-chromatography," Pure Appl. Chem. **63**, 71–80 (1991).
2. T. H. Margrain, M. Boulton, J. Marshall, and D. H. Sliney, "Do blue light filters confer protection against age-related macular degeneration?" Prog. Retinal Eye Res. **23**, 523–531 (2004).
3. J. M. Nolan, R. Power, J. Stringham, J. Dennison, J. Stack, D. Kelly, R. Moran, K. O. Akuffo, L. Corcoran, and S. Beatty, "Enrichment of macular pigment enhances contrast sensitivity in subjects free of retinal disease: central retinal enrichment supplementation trials–report 1," Invest. Ophthalmol. Vis. Sci. **57**, 3429–3439 (2016).
4. C. M. Putman and C. J. Bassi, "Macular pigment spatial distribution effects on glare disability," J. Optom. **8**, 258–265 (2015).
5. J. M. Stringham, E. R. Bovier, J. C. Wong, and B. R. Hammond, Jr., "The influence of dietary lutein and zeaxanthin on visual performance," J. Food Sci. **75**, R24–R29 (2010).
6. J. M. Stringham and B. R. Hammond, Jr., "The glare hypothesis of macular pigment function," Optom. Vis. Sci. **84**, 859–864 (2007).
7. V. M. Reading and R. A. Weale, "Macular pigment and chromatic aberration," J. Opt. Soc. Am. **64**, 231–234 (1974).
8. F. Khachik, P. S. Bernstein, and D. L. Garland, "Identification of lutein and zeaxanthin oxidation products in human and monkey retinas," Invest. Ophthalmol. Vis. Sci. **38**, 1802–1811 (1997).
9. B. R. Hammond, B. R. Wooten, and J. Curran-Celentano, "Carotenoids in the retina and lens: possible acute and chronic effects on human visual performance," Arch. Biochem. Biophys. **385**, 41–46 (2001).
10. M. Boulton, M. Rozanowska, and B. Rozanowski, "Retinal photodamage," J. Photochem. Photobiol. B **64**, 144–161 (2001).
11. D. M. Snodderly, J. D. Auran, and F. C. Delori, "The macular pigment II. Spatial distribution in primate retinas," Invest. Ophthalmol. Vis. Sci. **25**, 674–685 (1984).
12. E. Arnault, C. Barrau, C. Nanteau, P. Gondouin, K. Bigot, F. Vienot, E. Gutman, V. Fontaine, T. Villette, D. Cohen-Tannoudji, J. A. Sahel, and S. Picaud, "Phototoxic action spectrum on a retinal pigment epithelium model of age-related macular degeneration exposed to sunlight normalized conditions," PLoS ONE **8**, e71398 (2013).
13. N. K. Scripsema, D. N. Hu, and R. B. Rosen, "Lutein, zeaxanthin, and meso-zeaxanthin in the clinical management of eye disease," J. Ophthalmol. **2015**, 865179 (2015).
14. R. A. Bone, J. T. Landrum, S. T. Mayne, C. M. Gomez, S. E. Tibor, and E. E. Twaroska, "Macular pigment in donor eyes with and without AMD: a case-control study," Invest. Ophthalmol. Vis. Sci. **42**, 235–240 (2001).
15. J. Wu, E. Y. Cho, W. C. Willett, S. M. Sastry, and D. A. Schaumberg, "Intakes of lutein, zeaxanthin, and other carotenoids and age-related macular degeneration during 2 decades of prospective follow-up," JAMA Ophthalmol. **133**, 1415–1424 (2015).
16. A. Ozyurt, N. Kocak, P. Akan, O. G. Calan, T. Ozturk, M. Kaya, E. Karahan, and S. Kaynak, "Comparison of macular pigment optical density in patients with dry and wet age-related macular degeneration," Indian J. Ophthalmol. **65**, 477–481 (2017).
17. M. Trieschmann, G. Spital, A. Lommatzsch, E. van Kuijk, F. Fitzke, A. C. Bird, and D. Pauleikhoff, "Macular pigment: quantitative analysis on autofluorescence images," Graefe's Arch. Clin. Exp. Ophthalmol. **241**, 1006–1012 (2003).
18. S. Beatty, I. J. Murray, D. B. Henson, D. Carden, H. H. Koh, and M. E. Boulton, "Macular pigment and risk for age-related macular degeneration in subjects from a Northern European population," Invest. Ophthalmol. Vis. Sci. **42**, 439–446 (2001).
19. P. S. Bernstein, D. Y. Zhao, S. W. Wintch, I. V. Ermakov, R. W. McClane, and W. Gellermann, "Resonance Raman measurement of macular carotenoids in normal subjects and in age-related macular degeneration patients," Ophthalmology **109**, 1780–1787 (2002).
20. S. K. West, F. S. Rosenthal, N. M. Bressler, S. B. Bressler, B. Munoz, S. L. Fine, and H. R. Taylor, "Exposure to sunlight and other risk-factors for age-related macular degeneration," Arch. Ophthalmol. **107**, 875–879 (1989).
21. W. Smith, P. Mitchell, and S. R. Leeder, "Smoking and age-related maculopathy: The blue mountains eye study," Arch. Ophthalmol. **114**, 1518–1523 (1996).
22. M. K. M. Adams, J. A. Simpson, K. Z. Aung, G. A. Makeyeva, G. G. Giles, D. R. English, J. Hopper, R. H. Guymer, P. N. Baird, and L. D. Robman, "Abdominal obesity and age-related macular degeneration," Am. J. Epidemiol. **173**, 1246–1255 (2011).
23. E. J. Johnson, "Obesity, lutein metabolism, and age-related macular degeneration: a web of connections," Nutr. Rev. **63**, 9–15 (2005).
24. O. Howells, F. Eperjesi, and H. Bartlett, "Measuring macular pigment optical density in vivo: a review of techniques," Graefe's Arch. Clin. Exp. Ophthalmol. **249**, 315–347 (2011).
25. S. E. Temple, J. E. McGregor, C. Miles, L. Graham, J. Miller, J. Buck, N. E. Scott-Samuel, and N. W. Roberts, "Perceiving polarization with the naked eye: characterization of human polarization sensitivity," Proc. R. Soc. B **282**, 20150338 (2015).
26. R. A. Bone and J. T. Landrum, "Dichroism of lutein: a possible basis for Haidinger's brushes," Appl. Opt. **22**, 775–776 (1983).
27. J. McGregor, S. Temple, and G. Horvath, "Human polarization sensitivity," in *Polarized Light and Polarization Vision in Animal Sciences*, G. Horvath, ed., 2nd ed. (Springer-Verlag, 2014), pp. 303–315.
28. G. P. Misson, S. E. Temple, and S. J. Anderson, "Computational simulation of Haidinger's brushes," J. Opt. Soc. Am. A **35**, 946–952 (2018).
29. G. P. Misson, "Form and behavior of Haidinger's brushes," Ophthal. Physiol. Opt. **13**, 392–396 (1993).
30. G. P. Misson, "A Mueller matrix model of Haidinger's brushes," Ophthal. Physiol. Opt. **23**, 441–447 (2003).
31. M. Rothmayer, W. Dultz, E. Frins, Q. Zhan, D. Tierney, and H. Schmitzer, "Nonlinearity in the rotational dynamics of Haidinger's brushes," Appl. Opt. **46**, 7244–7251 (2007).

32. W. Grudzinski, L. Nierzwicki, R. Welc, E. Reszczynska, R. Luchowski, J. Czub, and W. I. Gruszecki, "Localization and orientation of xanthophylls in a lipid bilayer," Sci. Rep. **7**, 9619 (2017).
33. R. A. Bone, "The role of the macular pigment in the detection of polarized light," Vision Res. **20**, 213–220 (1980).
34. R. A. Bone and J. T. Landrum, "Macular pigment in Henle fiber membranes: a model for Haidinger's brushes," Vision Res. **24**, 103–108 (1984).
35. H. W. Forster, "The clinical use of the Haidinger's brushes phenomenon," Am. J. Ophthalmol. **38**, 661–665 (1954).
36. E. Myrowitz, "Recent explanation of Haidinger brushes and their clinical use," Am. J. Optom. Physiol. Opt. **56**, 305–308 (1979).
37. S. E. Temple, V. Pignatelli, T. Cook, M. J. How, T.-H. Chiou, N. W. Roberts, and N. J. Marshall, "High-resolution polarisation vision in a cuttlefish," Curr. Biol. **22**, R121–R122 (2012).
38. V. Pignatelli, S. E. Temple, T. H. Chiou, N. W. Roberts, S. P. Collin, and N. J. Marshall, "Behavioural relevance of polarization sensitivity as a target detection mechanism in cephalopods and fishes," Philos. Trans. R. Soc. London B **366**, 734–741 (2011).
39. W. K. Haidinger, "Über das direkte Erkennen des polarisierten Lichts und der Lage der Polarisationsebene," Ann. Phys. **139**, 29–39 (1844).
40. S. Magnussen, L. Spillmann, F. Sturzel, and J. S. Werner, "Unveiling the foveal blue scotoma through an afterimage," Vision Res. **44**, 377–383 (2004).
41. F. C. Delori, D. G. Goger, B. R. Hammond, D. M. Snodderly, and S. A. Burns, "Macular pigment density measured by autofluorescence spectrometry: comparison with reflectometry and heterochromatic flicker photometry," J. Opt. Soc. Am. A **18**, 1212–1230 (2001).
42. P. L. Muller, S. Muller, M. Gliem, K. Kupper, F. G. Holz, W. M. Harmening, and P. C. Issa, "Perception of Haidinger brushes in macular disease depends on macular pigment density and visual acuity," Invest. Ophthalmol. Vis. Sci. **57**, 1448–1456 (2016).
43. R. L. P. van der Veen, T. T. J. M. Berendschot, F. Hendrikse, D. Carden, M. Makridaki, and I. J. Murray, "A new desktop instrument for measuring macular pigment optical density based on a novel technique for setting flicker thresholds," Ophthal. Physiol. Opt. **29**, 127–137 (2009).
44. D. M. Snodderly, J. A. Mares, B. R. Wooten, L. Oxton, M. Gruber, T. Ficek, and C. M. P. S. Grp, "Macular pigment measurement by heterochromatic flicker photometry in older subjects: the carotenoids and age-related eye disease study," Invest. Ophthalmol. Vis. Sci. **45**, 531–538 (2004).
45. M. Sharifzadeh, P. S. Bernstein, and W. Gellermann, "Nonmydriatic fluorescence-based quantitative imaging of human macular pigment distributions," J. Opt. Soc. Am. A **23**, 2373–2387 (2006).
46. A. G. Robson, J. D. Moreland, D. Pauleikhoff, T. Morrissey, G. E. Holder, F. W. Fitzke, A. C. Bird, and F. van Kuijk, "Macular pigment density and distribution: comparison of fundus autofluorescence with minimum motion photometry," Vision Res. **43**, 1765–1775 (2003).
47. T. Berendschot and D. van Norren, "Macular pigment shows ringlike structures," Invest. Ophthalmol. Vis. Sci. **47**, 709–714 (2006).
48. S. Alassane, C. Binquet, L. Arnould, O. Fleck, N. Acar, C. Delcourt, L. Bretillon, A. M. Bron, and C. Creuzot-Garcher, "Spatial distribution of macular pigment in an elderly French population: the Montrachet study," Invest. Ophthalmol. Vis. Sci. **57**, 4469–4475 (2016).
49. R. O. Beirne, "The macular pigment optical density spatial profile and increasing age," Graefe's Arch. Clin. Exp. Ophthalmol. **252**, 383–388 (2014).
50. J. Loughman, G. Scanlon, J. M. Nolan, V. O'Dwyer, and S. Beatty, "An evaluation of a novel instrument for measuring macular pigment optical density: the MPS 9000," Acta Ophthalmol. **90**, e90–e97 (2012).
51. R. de Kinkelder, R. L. P. van der Veen, F. D. Verbaak, D. J. Faber, T. G. van Leeuwen, and T. Berendschot, "Macular pigment optical density measurements: evaluation of a device using heterochromatic flicker photometry," Eye **25**, 105–112 (2011).
52. A. O'Brien, C. Leahy, and C. Dainty, "Imaging system to assess objectively the optical density of the macular pigment in vivo," Appl. Opt. **52**, 6201–6212 (2013).
53. P. S. Bernstein, D. Y. Zhao, M. Sharifzadeh, I. V. Ermakov, and W. Gellermann, "Resonance Raman measurement of macular carotenoids in the living human eye," Arch. Biochem. Biophys. **430**, 163–169 (2004).
54. J. L. Dennison, J. Stack, S. Beatty, and J. M. Nolan, "Concordance of macular pigment measurements obtained using customized heterochromatic flicker photometry, dual-wavelength autofluorescence, and single-wavelength reflectance," Exp. Eye Res. **116**, 190–198 (2013).
55. H. Bartlett, L. Stainer, S. Singh, F. Eperjesi, and O. Howells, "Clinical evaluation of the MPS 9000 Macular Pigment Screener," Br. J. Ophthalmol. **94**, 753–756 (2010).
56. G. Y. Sui, G. C. Liu, G. Y. Liu, Y. Y. Gao, Y. Deng, W. Y. Wang, S. H. Tong, and L. Wang, "Is sunlight exposure a risk factor for age-related macular degeneration? A systematic review and meta-analysis," Br. J. Ophthalmol. **97**, 389–394 (2013).
57. W. T. Ham, H. A. Mueller, and D. H. Sliney, "Retinal sensitivity to damage from short wavelength light," Nature **260**, 153–155 (1976).
58. W. T. Ham, J. J. Ruffolo, H. A. Mueller, A. M. Clarke, and M. E. Moon, "Histologic analysis of photochemical lesions produced in rhesus retina by short-wavelength light," Invest. Ophthalmol. Vis. Sci. **17**, 1029–1035 (1978).
59. J. E. Roberts, "Ultraviolet radiation as a risk factor for cataract and macular degeneration," Eye Contact Lens **37**, 246–249 (2011).
60. B. M. J. Merle, B. Buaud, J. F. Korobelnik, A. Bron, M. N. Delyfer, M. B. Rougier, H. Savel, C. Vaysse, C. Creuzot-Garcher, and C. Delcourt, "Plasma long-chain omega-3 polyunsaturated fatty acids and macular pigment in subjects with family history of age-related macular degeneration: the Limpia Study," Acta Ophthalmol. **95**, e763–e769 (2017).
61. M. Dietzel, M. Zeimer, B. Heimes, B. Claes, D. Pauleikhoff, and H. W. Hense, "Determinants of macular pigment optical density and its relation to age-related maculopathy: results from the Muenster Aging and Retina Study (MARS)," Invest. Ophthalmol. Vis. Sci. **52**, 3452–3457 (2011).
62. J. M. Nolan, J. Stack, O. O. Donovan, E. Loane, and S. Beatty, "Risk factors for age-related maculopathy are associated with a relative lack of macular pigment," Exp. Eye Res. **84**, 61–74 (2007).
63. B. R. Hammond and M. Caruso-Avery, "Macular pigment optical density in a southwestern sample," Invest. Ophthalmol. Vis. Sci. **41**, 1492–1497 (2000).
64. M. L. Kirby, S. Beatty, J. Stack, M. Harrison, I. Greene, S. McBrinn, P. Carroll, and J. M. Nolan, "Changes in macular pigment optical density and serum concentrations of lutein and zeaxanthin in response to weight loss," Br. J. Nutr. **105**, 1036–1046 (2011).
65. E. A. Boettner and J. R. Wolter, "Transmission of the ocular media," Invest. Ophthalmol. Vis. Sci. **1**, 776–783 (1962).

137.222.190.173 {ts '2019-05-31 11:32:47'}